

## TECHNICAL NOTE

Serge-Étienne Parent,<sup>1</sup> Alexandre Cabral,<sup>2</sup> Eduardo Dell'Avanzi,<sup>3</sup> and Jorge G. Zornberg<sup>4</sup>

# Determination of the Hydraulic Conductivity Function of a Highly Compressible Material Based on Tests with Saturated Samples

**ABSTRACT:** An alternative procedure to determine the hydraulic conductivity function ( $k$ -function) based on relationships between saturated hydraulic conductivity and void ratio and between air-entry value and void ratio is proposed. The procedure was applied to determine the  $k$ -function of deinking by-products, a highly compressible industrial by-product that is used as alternative material in geoenvironmental applications. The validity of the procedure is verified by comparing the  $k$ -function of a compressible soil obtained based on the proposed procedure (using published experimental data) with experimentally determined unsaturated hydraulic conductivities for the same soil.

**KEYWORDS:** hydraulic conductivity function, compressible soils, suction, characteristic curve, deinking by-products

### Introduction

Because of experimental difficulties for direct measurement of the unsaturated hydraulic conductivity of porous materials, current practice involves estimation from water retention curve (WRC) models (Mualem 1976; Fredlund and Xing 1994; Huang et al. 1998; Fredlund 2002). Consequently, the reliability of the hydraulic conductivity function ( $k$ -function) depends not only on the accuracy of the WRC, but also on the model used for its indirect determination. This study presents a procedure to determine the  $k$ -function of highly compressible materials, based on hydraulic conductivity tests performed on saturated samples and on suction test data performed in order to obtain the air-entry value. Suction tests must be done so that volume changes can be monitored using methodologies such as proposed by Cabral et al. (2004). The validity of the procedure is verified by comparing results of actual unsaturated hydraulic conductivity tests (published experimental data for a compressible soil) with predictions made by applying the procedure.

### Materials and Methods

Deinking by-products (DBP) are produced in the early stages of the paper recycling process. The main inorganic components of this material are calcite, meta-kaolinite, and rutile, whereas cellulose, hemicellulose, and lignine are the main organic components (Cabral et al. 2002). Laboratory tests have shown that the consolidation behavior of DBP resembles that of highly organic materials, insofar as it presents a significant secondary consolidation (creep) phase.

Received January 2, 2003; accepted for publication May 12, 2004; published November 2004.

<sup>1</sup> Ph.D. candidate, Dept. Civil Eng., Univ. de Sherbrooke, Quebec, Canada.

<sup>2</sup> Professor, Dept. Civil Eng., Univ. de Sherbrooke, Sherbrooke, Quebec, Canada.

<sup>3</sup> Assistant Professor, Dept. Civil Eng., Federal University of Paraná, Brazil.

<sup>4</sup> Assistant Professor, Dept. Civil Eng., University of Texas at Austin.

Saturated hydraulic conductivity tests performed in oedometers after each of several consolidation steps show that the saturated hydraulic conductivity for this material lies in the range of  $5 \times 10^{-10}$  m/s and  $5 \times 10^{-9}$  m/s (Burnotte et al. 2000). The results of several tests, reproduced in Fig. 1, show a linear relationship between the logarithm of the saturated hydraulic conductivity and void ratio. This relationship can be expressed as follows:

$$k_{sat} = k'_{sat} 10^{b(e-e')} \quad (1)$$

where  $k_{sat}$  is the saturated hydraulic conductivity for a void ratio  $e$ ,  $e'$  is an arbitrary reference void ratio,  $k'_{sat}$  is the saturated hydraulic conductivity at  $e'$ , and  $b$  is the slope of the  $\log(k_{sat})$  versus  $e$  relationship (Fig. 1).

Based on experimental data reported in the literature (e.g., Laliberte et al. 1966), Huang et al. (1998) assumed—and presented evidence—that the logarithm of the air-entry value ( $\psi_{aev}$ ) is linearly proportional to the void ratio at the air-entry value ( $e_{aev}$ ). That is:

$$\log\left(\frac{\psi_{aev}}{\psi'_{aev}}\right) = \varepsilon(e_{aev} - e'_{aev}) \quad (2)$$

where  $\psi_{aev}$  is the air-entry value for void ratio  $e_{aev}$ ,  $\psi'_{aev}$  is the air-entry value at the arbitrary reference void ratio  $e'_{aev}$ , and  $\varepsilon$  is the slope of the  $\log(\psi_{aev})$  versus  $e_{aev}$  curve.

In the present study, the  $\psi_{aev}$  values were obtained from suction tests performed with DBP whose main goals were to determine the WRC of this material and the air-entry value. The methodology employed, that allows for consideration of volume changes during testing, is described in Cabral et al. (2004). In the cases where a 0-bar porous stone was employed (i.e., a porous stone with a negligible capacity to prevent air from breaking through it), the  $\psi_{aev}$  was considered to be equal to the suction value where air broke through the sample. In the cases where 1-bar porous stones were employed, the  $\psi_{aev}$  was considered to be equal to the suction value where significant loss of water was observed, i.e., in the region

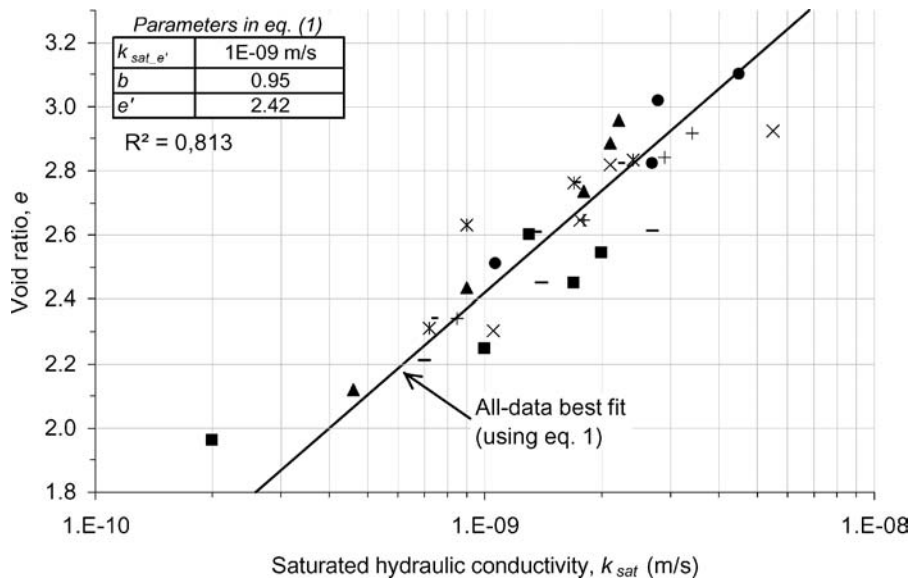


FIG. 1—Void ratio as a function of saturated hydraulic conductivity for deinking by-products.

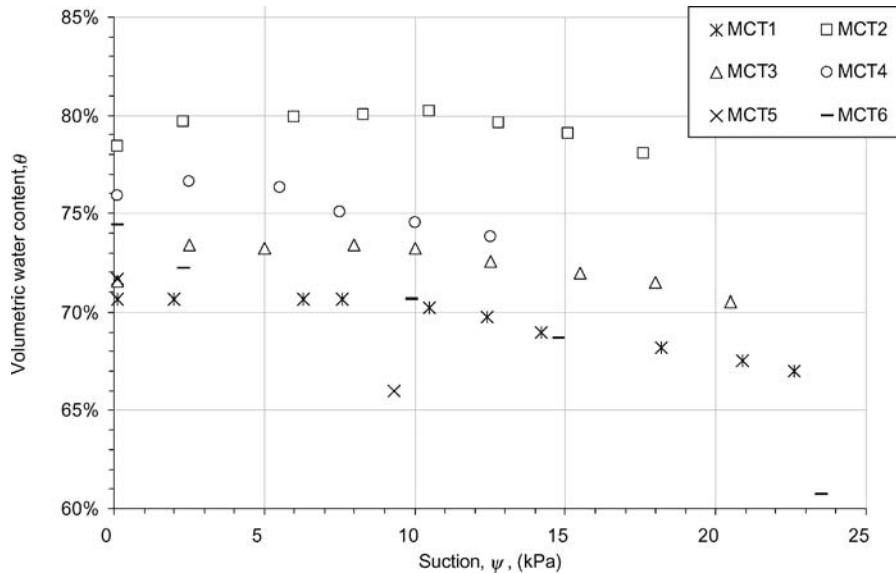


FIG. 2—Water retention curves up to the air-entry value for deinking by-products consolidated to different void ratios.

of the inflection point determined using the procedure proposed by Fredlund and Xing (1994). Figure 2 shows results from various suction tests performed with DBP with different initial void ratios. The air-entry values were coupled with their corresponding void ratio in order to obtain Fig. 3, that shows that the relationship between  $\log(\psi_{aev})$  and  $e_{aev}$  is approximately linear, which is consistent with Eq 2.

### Conceptual Model

Figure 4 can be utilized to explain the concept behind the proposed model. The  $k$ -function is described here by two curves. The first (denoted as Curve 1) describes how the saturated hydraulic conductivity varies with suction for a sample of a highly compressible material consolidated to an initial void ratio  $e_{0-i}$ . Using a void ratio function ( $e$ -function; proposed later), it is possible to predict the void ratio  $e_i$  for any suction value  $\psi$  and, using Eq 1, to predict

the saturated hydraulic conductivity,  $k_{sat-i}$ , corresponding to  $e_i$  and  $\psi$ . Using Eq 2 and the  $e$ -function, the air-entry value for Test  $i$ ,  $\psi_{aev-i}$ , is then determined. The void ratio corresponding to  $\psi_{aev-i}$  is  $e_{aev-i}$ .

The second curve (denoted as Curve 3 in Fig. 4) can also be estimated based on saturated hydraulic conductivity tests and the WRC. For the same Test  $i$  as above, consolidated to an initial void ratio  $e_{0-i}$ , when suction exceeds  $\psi_{aev-i}$ , the void ratio decreases to a value  $e_{unsat-i}$  lower than  $e_{aev-i}$ . Accordingly, the associated hydraulic conductivity decreases—as expected—to a value  $k_{unsat-i}$  lower than  $k_{sat-i}$ . This new hydraulic conductivity value,  $k_{unsat-i}$ , corresponds to the unsaturated hydraulic conductivity for Sample  $i$  when its void ratio is  $e_{unsat-i}$ .

According to Eq 1, it is possible to obtain a saturated hydraulic conductivity corresponding to a void ratio  $e_{unsat-i}$ . In this case, another Test  $ii$  (Curve 2 in Fig. 4) must be performed using the same material, but the sample is consolidated to an initial void ratio

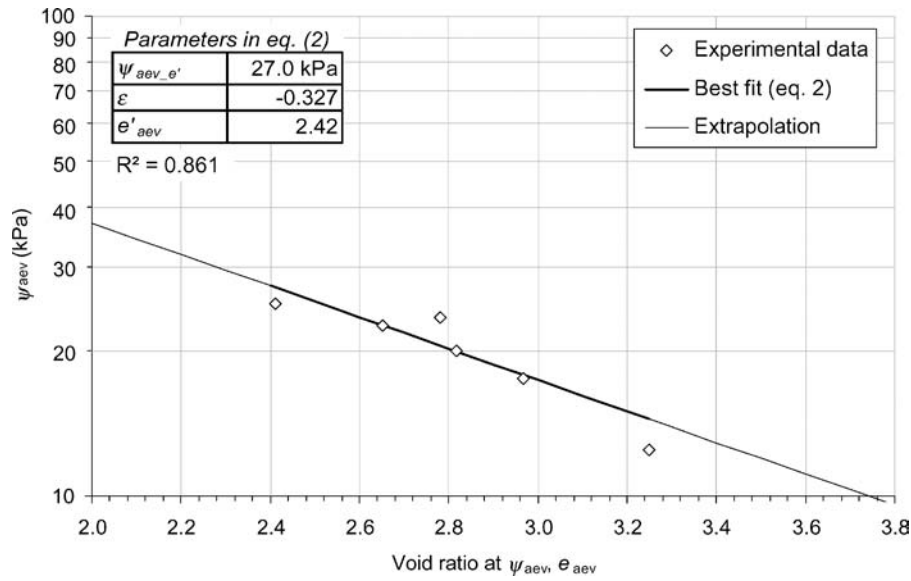


FIG. 3—Air-entry value as a function of void ratio for deinking by-products.

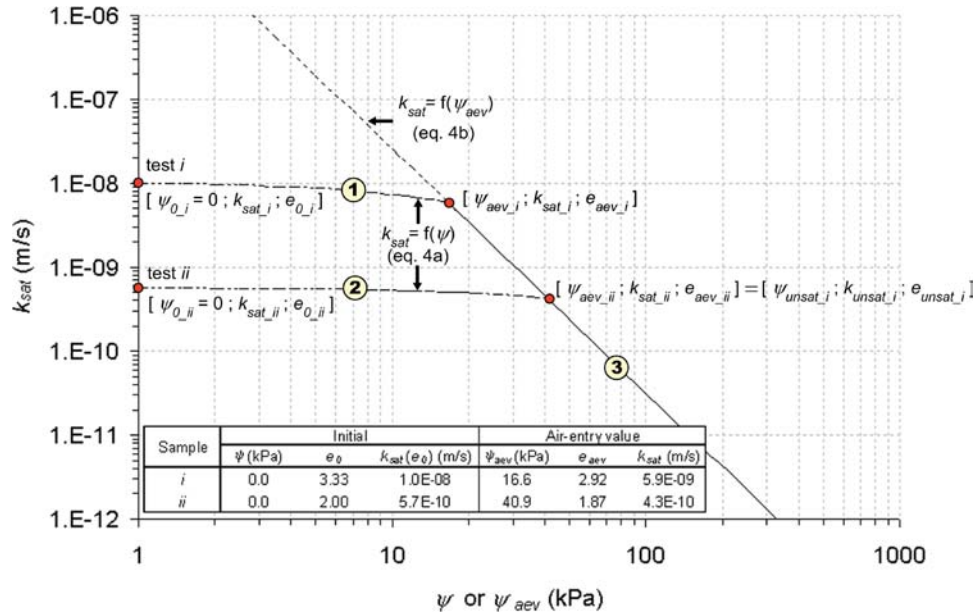


FIG. 4—Saturated hydraulic conductivity as a function of air-entry value for deinking by-products.

$e_{0_{ii}} < e_{0_{i}}$ . Suction is then applied to bring the sample to a void ratio  $e_{aev_{ii}}$  equal to  $e_{unsat_{i}}$  (Fig. 4).

Given that, as shown schematically in Fig. 5a, various WRC superimpose into a single virgin desaturation branch (Toll 1988) (this is equivalent to the consolidation behavior of clayey soils) and that the slope of the  $k$ -function can be calculated from the slope of the WRC, it may be inferred that  $k$ -functions also superimpose onto the same curve. Therefore, the curve obtained by joining the points  $(\psi_{aev}; k_{sat})$  for tests  $i, ii$ , etc., i.e., Curve 3 in Fig. 4, would describe the  $k$ -function of the compressible material for suctions greater than the air-entry value.

### Proposed Procedure

In order to model Curve 1 in Fig. 4, an  $e$ -function must first be defined. The following model is proposed to describe the suction-

induced shrinkage behavior of DBP,

$$e_i = e_c + (e_{0_{i}} - e_c)(1 + e_{0_{i}}c_1\psi)^{c_2} \quad (3)$$

where  $e_i$  is the void at Suction  $\psi$ , and  $c_1$  and  $c_2$  are fitting parameters. The parameter  $e_c$  is the convergence void ratio, i.e., the void ratio at which the  $e$  versus  $\psi$  curves, obtained from suction tests with various representative samples, converge. The curves and fitting parameters obtained are presented in Fig. 5b. Although the curve in this figure extends beyond the air-entry value, obtaining  $e$  versus  $\psi$  curve beyond the air-entry value is not necessary for the purpose of determining Curve 1 in Fig. 4. This is due to the fact that the value of  $e_c$  does not affect significantly the value of  $e_i$  for suctions lower than  $\psi_{aev_{i}}$ , whether it is determined by a least square optimization technique or simply imposed based on a known residual value (as is the case in Fig. 5b).

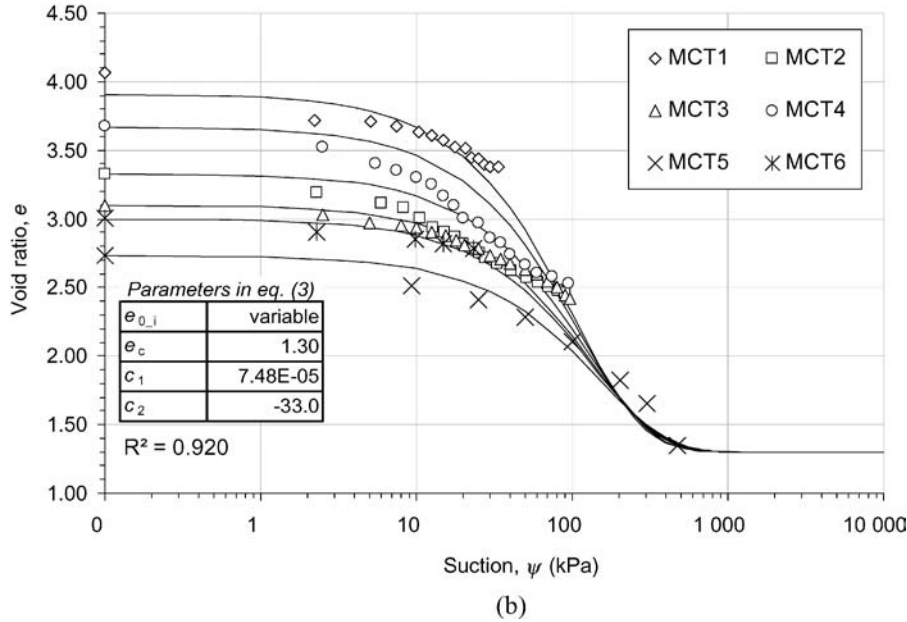
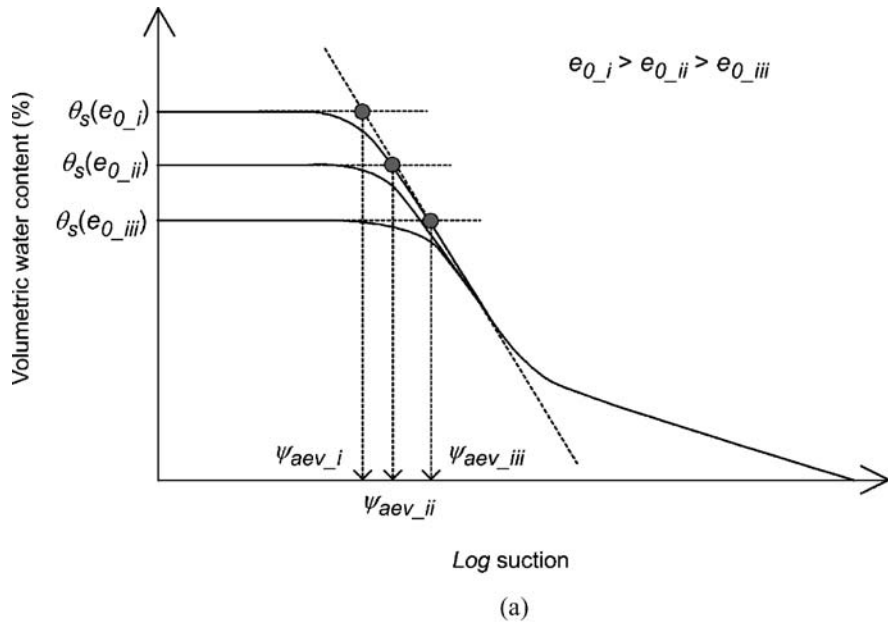


FIG. 5—Water retention curves for a material consolidated to different initial void ratios (a); Void ratio function for deinking by-products (b).

By substituting  $e$  in Eq 1 by  $e_i$  obtained from Eq 3, the following model for Curve 1 (or Curve 2) is obtained:

$$k_{sat-i} = k'_{sat} 10^{b(e_c + (e_{0_i} - e_c)(1 + e_{0_i} c_1 \psi)^2 - e'_{aev})} \quad \text{for } \psi < \psi_{aev-i} \quad (4a)$$

Curve 3 (Fig. 4) is obtained by replacing the parameters  $e$  and  $e'$  in Eq 1 by, respectively,  $e_{aev}$  and  $e'_{aev}$ , by isolating  $e_{aev}$  in Eq 2 and finally by substituting Eq 2 into Eq 1. Equation 4b is then used to establish a linear relationship on a *log-log* scale between the saturated hydraulic conductivity and  $\psi_{aev}$ :

$$k_{sat} = k'_{sat} \left( \frac{\psi_{aev}}{\psi'_{aev}} \right)^{b/\varepsilon} \quad \text{for } \psi_{aev} > \psi_{aev-i} \quad (4b)$$

### Validation and Discussion

In order to validate the proposed procedure, Eqs 3 and 4 were applied to experimental data published by Huang et al. (1998). The results, presented in Fig. 6, are compared to unsaturated hydraulic conductivity measurements, also reported by Huang et al. (1998).

Hydraulic conductivity, suction, and void ratio values obtained from flexible-wall permeability tests allowed for the determination of the parameters in Eq 4a. Parameters  $\psi'_{aev}$  and  $\varepsilon$  were obtained using results of pressure-plate cell tests, from which the curve  $\log(\psi_{aev})$  versus  $e_{aev}$  could in turn be determined.

There seems to be a better agreement between rigid-wall hydraulic conductivity tests (triangles in Fig. 6) and the curve obtained by applying Eq 4. Up to 30 kPa of suction, a good agreement also exists with results from flexible-wall hydraulic conductivity tests (squares in Fig. 6). The all-data best fit, which was determined by a least-squares minimization approach using actual unsaturated

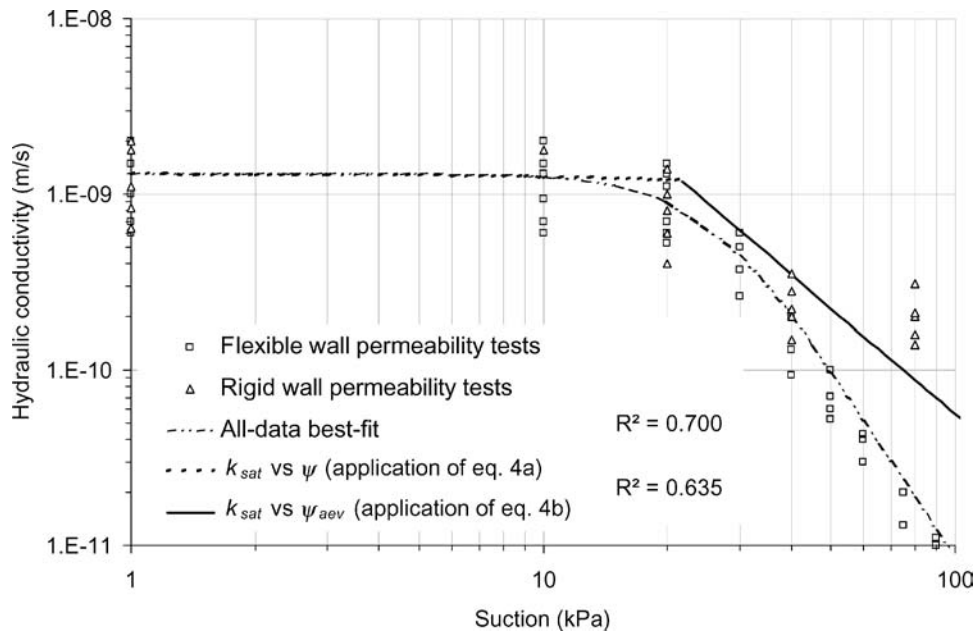


FIG. 6—Hydraulic conductivity as a function of suction (data from Huang et al. 1998).

hydraulic conductivity tests, was compared to the curve obtained by applying Eq 4. It can be observed in Fig. 6 that the differences between the proposed procedure and the all-data best fit are relatively minor up to  $\psi_{aev-i}$  and much less than one order of magnitude for suctions greater than  $\psi_{aev-i}$ . This suggests that the determination of the  $k$ -function can be made based on known relationships between  $k_{sat}$  and void ratio, and  $\psi_{aev}$  and void ratio with reasonable confidence.

### Conclusions

A procedure to determine the  $k$ -function based on the relationships between saturated hydraulic conductivity and void ratio, and between air-entry value and void ratio was proposed and applied to a highly compressible material (deinking by-products). A comparison between the  $k$ -function obtained by applying this procedure to experimental data reported in the literature (for a Saskatchewan silty sand) and actual unsaturated hydraulic conductivity data for the same silty sand shows a good agreement up to a suction value in the vicinity of 30 kPa. For greater suctions, a reasonable agreement (less than one order of magnitude) is still obtained.

The use of the proposed procedure to determine the  $k$ -function requires suction and saturated hydraulic conductivity testing on samples consolidated to different initial void ratios. However, these tests are more expeditious than direct determination of  $k$ -functions. Hence, the  $k_{sat} - \psi_{aev}$  procedure may be a valuable and cost-effective solution in many situations.

### Acknowledgments

Funding for this study was provided in part by Industries Cascades, Inc., Perkins Papers, Ltd., and NSERC (Canada) under the University-Industry partnership grant number CRD 192179 and the first author Discovery Grant (NSERC). Support received by the second author from the CNPq (Brazil) and from the National Science Foundation by the last author is also greatly appreciated.

### References

- Burnotte, F. G., Lefebvre, A., Cabral, C. A., and Veilleux, A., 2000, "Use of Deinking Residues for the Final Cover of a MSW Landfill," Vol. 53e, *Conférence Canadienne de Géotechnique*, Montreal, pp. 585–591.
- Cabral, A., Burnotte, F., Lefebvre, G., and Panarotto, C. T., 2002, "Geotechnical Characterization of a Pulp and Paper Residue to be Used as Alternative Cover Material to Landfill and to Acid Generating Tailings," *Proceedings of the 4th International Congress on Environmental Geotechnics*, Rio de Janeiro, Brazil, pp. 207–212.
- Cabral, A. R., Planchet, L., Marinho, F. A., and Lefebvre, G., 2004, "Determination of the Soil Water Characteristic Curve of Highly Compressible Materials: Case Study of Pulp and Paper By-Product," *Geotechnical Testing Journal*, Vol. 27, pp. 154–162.
- Fredlund, D. G., 2002, "Use of Soil-Water Characteristic Curve in the Implementation of Unsaturated Soil Mechanics," *Proceedings of the 3rd International Conference on Unsaturated Soils*, Recife, Brazil.
- Fredlund, D. G. and Xing, A. Q., 1994, "Equations for the Soil-Water Characteristic Curve," *Canadian Geotechnical Journal*, Vol. 31, pp. 521–532.
- Huang, S. Y., Barbour, S. L., and Fredlund, D. G., 1998, "Development and Verification of a Coefficient of Permeability Function for a Deformable Unsaturated Soil," *Canadian Geotechnical Journal*, Vol. 35, pp. 411–425.
- Labiberte, G. E., Corey, A. T., and Brooks, R. H., 1966, "Properties of Unsaturated Porous Media," Hydrology Paper No. 17, Colorado State University, Fort Collins, CO.
- Mualem, Y., 1976, "A New Model for Predicting the Hydraulic Conductivity of Unsaturated Porous Media," *Water Resources Research*, Vol. 12, pp. 513–522.
- Toll, D. G., 1988, "The Behaviour of Unsaturated Compacted Naturally Occurring Gravel," Ph.D. Thesis, University of London, London.